New places and phases of CO-poor/C I-rich molecular gas in the Universe

Padelis P. Papadopoulos,[1,2,3]⋆ Thomas G. Bisbas[4,5]⋆ and Zhi-Yu Zhang[6,7]

[1]*Department of Physics, Section of Astrophysics, Astronomy and Mechanics, Aristotle University of Thessaloniki, Thessaloniki, GR-54124, Greece*
[2]*Research Center for Astronomy, Academy of Athens Soranou Efesiou 4, GR-11527, Athens, Greece*
[3]*School of Physics and Astronomy, Cardiff University, Queen's Buildings, The Parade, Cardiff, CF24 3AA, UK*
[4]*Department of Astronomy, University of Virginia, Charlottesville, VA 22904, USA*
[5]*Max-Planck-Institut für Extraterrestrische Physik, Giessenbachstrasse 1, D-85748 Garching, Germany*
[6]*Institute for Astronomy, University of Edinburgh, Royal Observatory, Edinburgh, EH9 3HJ, UK*
[7]*European Southern Observatory, Headquarters, Karl-Schwarzschild-Strasse 2, D-85748, Garching bei München, Germany*

ABSTRACT

In this work, we extend the work on the recently discovered role of Cosmic Rays (CRs) in regulating the average CO/H_2 abundance ratio in molecular clouds (and thus their CO line visibility) in starburst galaxies, and find that it can lead to a CO-poor/C I-rich H_2 gas phase even in environments with Galactic or in only modestly enhanced CR backgrounds expected in ordinary star-forming galaxies. Furthermore, the same CR-driven astro-chemistry raises the possibility of a widespread phase transition of a molecular gas towards a CO-poor/CI-rich phase in: (a) molecular gas outflows found in star-forming galaxies, (b) active galactic nuclei (AGNs), and (c) near synchrotron-emitting radio jets and the radio-loud cores of powerful radio galaxies. For main sequence galaxies we find that CRs can render some of their molecular gas mass CO-invisible, compounding the effects of low metallicities. Imaging the two fine structure lines of atomic carbon with resolution high enough to search beyond the CI/CO-bright line regions associated with central starbursts can reveal such a CO-poor/C I-rich molecular gas phase, provided that relative brightness sensitivity levels of $T_b(\text{C I } 1-0)/T_b(\text{CO } J = 1-0)$ ~ 0.15 are reached. The capability to search for such gas in the Galaxy is now at hand with the new high-frequency survey telescope *HEAT* deployed in Antarctica and future ones to be deployed in Dome A. *ALMA* can search for such gas in star-forming spiral discs, galactic molecular gas outflows, and the CR-intense galactic and circumgalactic gas-rich environments of radio-loud objects.

Key words: astrochemistry – radiative transfer – methods: numerical – cosmic rays – photodissociation region (PDR) – galaxies: ISM.

1 INTRODUCTION

The utility of CO and its low-J rotational transitions as effective tracers of H_2 gas mass is now well-established observationally (e.g. Young & Scoville 1991; Solomon, Downes & Radford 1992; Solomon et al. 1997) and theoretically (e.g. Dickman, Snell & Schloerb 1986; Maloney & Black 1988; Bryant & Scoville 1996), provided: (a) the so-called $X_{CO}(= M(H_2)/L_{CO})$ factor is used only for $M(H_2) \geq 10^5 \, M_\odot$ (so that its statistical notion remains valid) and (b) the [CO]/[H_2] abundance ratio does not fall much below its average Galactic value of $\sim 10^{-4}$. The latter can happen in low-metallicity interstellar medium (ISM) with strong ambient far-ultraviolet (FUV) radiation fields (Pak et al. 1998; Bolatto,

Jackson & Ingalls 1999), such as those expected in metal-poor dwarf galaxies, leaving large amounts of H_2 gas as CO-invisible (Madden et al. 1997; Shi et al.). In the Milky Way and other ordinary spirals, this is expected also for molecular gas at large galactocentric distances where metallicity falls to $\sim 0.2 Z_\odot$ and much of the H_2 gas can be rendered (CO line)-invisible by the FUV-induced destruction of CO (Papadopoulos, Thi & Viti 2002; Wolfire, Hollenbach & McKee 2010).

It was only recently that Cosmic Rays (CRs) have been identified as a potentially more effective CO-destruction agent in molecular clouds compared to FUV photons (Bialy & Sternberg 2015; Bisbas, Papadopoulos & Viti 2015; Bisbas et al. 2017). Unlike the latter whose propagation (and thus CO-dissociation capability) is blunted by the strong dust absorption of FUV light taking place in the dust-rich HI phase and in outer H_2 cloud envelopes, CR-induced chemistry destroys CO volumetrically throughout a molecular cloud

irrespective of dust column. Other observational signatures of CR-controlled versus FUV-controlled chemistry of H_2 clouds in galaxies, (even when CO remains abundant) have been discussed thoroughly in the literature (e.g. Papadopoulos 2010; Meijerink et al. 2011), and will not concern us here. We should, nevertheless, mention that it is CRs that make the C II distribution concomitant with that of CO in H_2 gas clouds, rather existing only in a thin transition layer between C II-rich outer and CO-rich inner H_2 cloud regions {as the traditional photodissociation regions (PDR) view would have it, e.g. Hollenbach & Tielens 1999}. This makes C I lines equally good and more straightforward H_2 gas mass tracers as low-J CO lines, even under conditions where CO remains abundant in H_2 gas clouds.

A last theoretical effort to retain the PDR picture against the failure of its basic prediction of a C II/C I/CO stratification of species on the surface of FUV-illuminated H_2 clouds was made by introducing density inhomogeneities on the classic PDR picture (Meixner & Tielens 1993; Spaans & van Dishoeck 1997). There, the C II/C I/CO species stratification remained but only on small H_2 clumps while C I appeared spatially extended deeper into FUV-illuminated CO-rich inhomogeneous H_2 clouds. However, while CO-rich H_2 clumps of low filling factor, each with a C I 'coating', could reproduce the astonishing spatial correspondence between C I and ^{12}CO, ^{13}CO line emission observed in Giant Molecular Clouds (GMCs) across a wide range of conditions, they could not account for the tight intensity correlation between ^{12}CO, ^{13}CO (1–0), (2–1), and C I 1–0 line intensities, unless one postulates also a very standard H_2 clump making up all H_2 clouds, with characteristics that remain invariant across the wide range of ISM conditions (see Papadopoulos, Thi & Viti 2004, for details). CRs are the simplest and the most likely culprits in creating a volumetric rather than surface-like C I distribution in H_2 clouds, and therein lies the most notable difference between FUV-driven chemistry and gas thermal state, and a CR-driven one.

Another key difference between the two mechanisms besides their spatially distinct ways to destroy CO is that FUV-induced CO destruction leaves behind C I and C II, while CR-induced destruction yields mostly C I, provided that $T_{kin} \lesssim 50\,K$, otherwise CO abundance increases via the OH channel (Bisbas et al. 2017). This makes CR-induced CO-poor H_2 gas more accessible to observations via the two fine structures of atomic carbon at rest frequencies $\nu_{rest}^{CI}(1-0) \sim 492\,GHz\ ^3P_1 - {}^3P_0$ (hereafter 1–0) and $\nu_{rest}^{CI}(2-1) \sim 809\,GHz\ ^3P_2 - {}^3P_1$ (hereafter 2–1) than FUV-irradiated clouds. These [C I] lines can be observed over a large redshift range, starting from $z \sim 0$ to $z \sim 5$ for [C I] 1–0, and from $z \sim 0$ to $z \sim 8$ for [C I] 2–1, using ground-based telescopes, such as *ALMA* on the Atacama Desert Plateau, while the [C II] fine structure line, even if typically much brighter than the [C I] lines for warm gas, will be faint for cold H_2 gas ($T_k \sim (15 - 20)\,K$, while $E_{ul}(C\,II)/k_B \sim 92\,K$) away from star-forming (SF) sites. Moreover C II has a rest frequency of $\sim 1900\,GHz$, making it accessible to ground-based observations only once $z \gtrsim 2$, still extremely challenging until $z \gtrsim 4$. This leaves most of the star-formation history of the Universe (and its gas-fueling) outside the reach of [C II].

In this paper, we study the effects of a CR-regulated [CO/C I] average abundance in a low-density molecular gas in the Galaxy, the outer regions of local spirals, and distant main sequence (MS) galaxies. We conclude this work by examining the possibility of a CO-poor/C I-rich molecular gas in the CR-intense environments of molecular gas outflows from starbursts, and the environments of radio-loud objects.

2 LOW-DENSITY MOLECULAR GAS IN THE UNIVERSE: THE EFFECTS OF CRS

The CR effects on the relatively low-density molecular gas $\{N(H_2) \sim 50\text{-}500\,cm^{-3}\}$ have not been studied in detail, but early hints that CO can be effectively destroyed in such gas even at Galactic levels of CR energy densities exist (Bisbas et al. 2015). A low-density molecular gas phase can be found in a variety of places in the Universe, the nearest ones being the envelopes of ordinary GMCs in the Galaxy. Should their CO-marker molecule be wiped out by CRs, it would leave the corresponding H_2 gas mass CO-invisible, yielding a systematic underestimate of H_2 gas mass even in places where CO was considered an effective H_2 tracer. This is of particular importance since a typical log-normal distribution of $M(H_2)$-$n(H_2)$ expected in turbulent GMCs would place most of their total mass at densities of $N(H_2) < 500\,cm^{-3}$ (Padoan & Nordlund 2002). Moreover, CRs can act on the chemistry of H_2 gas as fast as the photon-driven processes driven by FUV radiation fields.

2.1 The Milky Way

Studies of the H I→H₂ phase transition in the metallicity and radiation environment of the Milky Way showed that it can commence from densities as low as $N(H_2) \sim 5\text{–}20\,cm^{-3}$, depending on the H_2 formation rate on grains and ambient dust shielding (Papadopoulos et al. 2002), while for density enhancements reaching above $N(H_2) \sim 50\,cm^{-3}$ this transition is complete (Jura 1975a,b; van Dishoeck & Black 1986; Shaya & Federman 1987; Andersson & Wannier 1993; Shull et al. 2000; Offner et al. 2013; Bialy, Burkhart & Sternberg 2017). However CO (and HCN) multi-J observations of Molecular Clouds (MCs) in the Galaxy, typically yield densities of $N(H_2) \sim 500\text{–}10^4\,cm^{-3}$ (Sakamoto et al. 1997; Heyer & Dame 2015; Bialy & Sternberg 2016). Thus, there is a significant range of gas densities $N(H_2) \sim 50\text{–}500\,cm^{-3}$ where Cold Neutral Medium gas can be molecular but perhaps not (CO-line)-bright, reminiscent of the translucent clouds (van Dishoeck & Black 1986).

Fig. 1 shows the column density maps of H I, H_2 CO, C I, C II, and T_{kin} distributions within inhomogeneous low-density gas clouds using the fractal rendering and thermo-chemical calculations presented by Bisbas et al. (2017) and using the 3D-PDR code[1] (Bisbas et al. 2012), but now subjected only to Galactic levels of interstellar radiation field and CR energy density (i.e. $\zeta' = 1$, where $\zeta' = \zeta_{CR}/10^{-17}\,s^{-1}$ and $G_\circ = 1$ normalized according to Draine 1978). The GMCs were constructed using the method described in Walch et al. (2015) for a fractal dimension of $\mathcal{D} = 2.4$ and assuming a mass of $M = 7 \times 10^4\,M_\odot$ but with different radial extent corresponding to three average number densities i.e. $\langle n \rangle \sim 50$, 100, and $200\,cm^{-3}$. We find that the maximum visual extinction, A_V, along the line-of-sight of these clouds is ~ 14, 22, and 40 mag, respectively. These GMCs have much smaller average number densities than the GMC studied in Bisbas et al. (2017) ($\langle n \rangle \sim 760\,cm^{-3}$). Furthermore, our computations are made for metallicities of both $Z = Z_\odot$ and $Z = 0.2Z_\odot$ representing the ISM for inner and the outer parts of the Milky Way.

From the maps in Fig. 1 it can be readily seen that for $\langle n \rangle \sim (50 - 100)\,cm^{-3}$ the H_2 gas can be rendered very CO-poor, even at Galactic levels of CR energy density, while for low metallicities this remains so up to $\langle n \rangle \sim 200\,cm^{-3}$ (the highest average

---

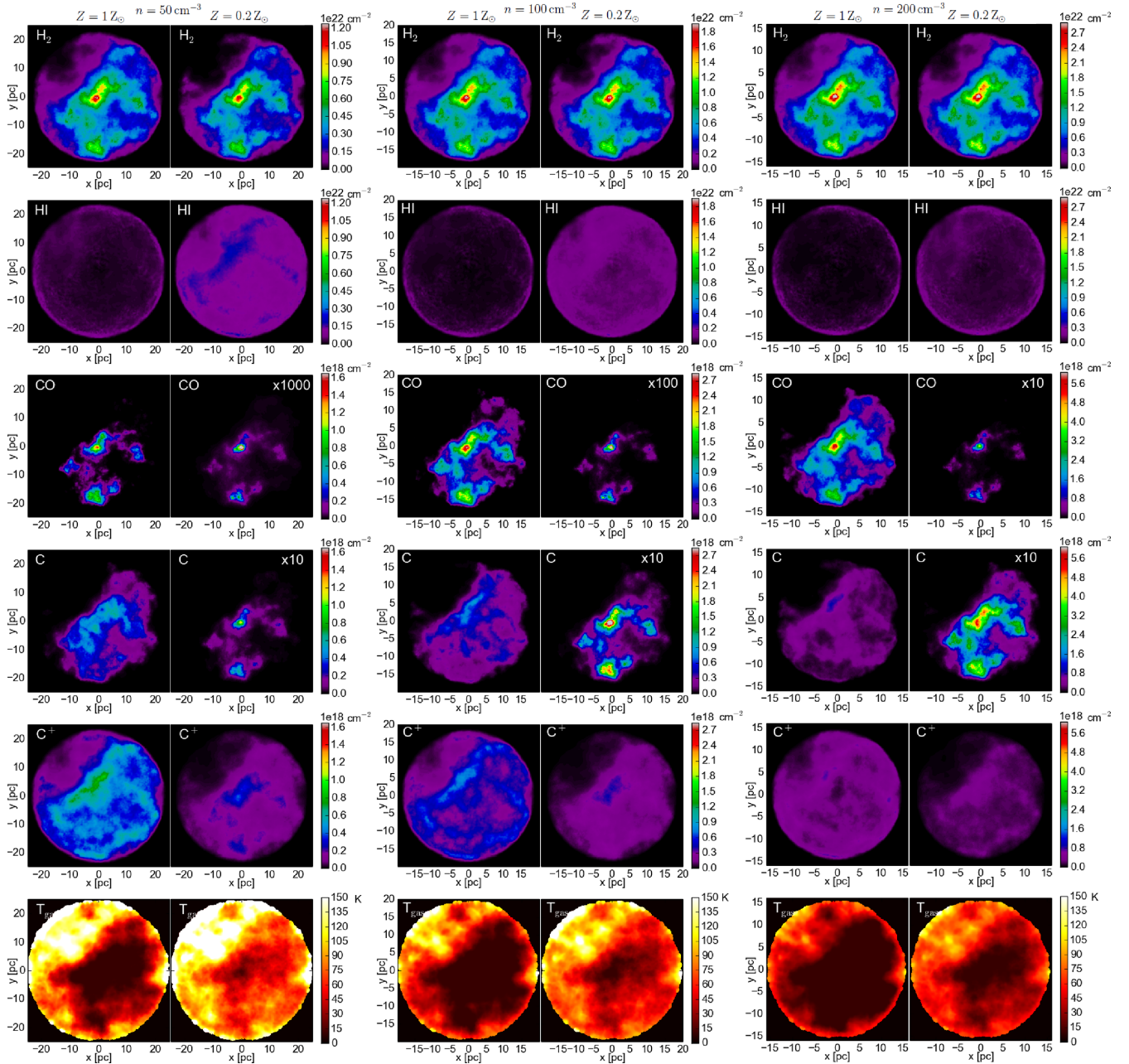[1] https://uclchem.github.io/

Figure 1. Column density (N) plots of H_2 (top row), $H\,I$ (second row), CO (third row), $C\,I$ (fourth row), $C\,II$ (fifth row) in different volume H_2 densities and metallicities. The colour bar has units of cm^{-2} and the axes have units of pc. The bottom row shows cross-sections of the gas temperature at the $z = 0$ pc plane. The colour bar there has units of K. The first two columns correspond to the GMC with $\langle n \rangle \sim 50\,cm^{-3}$, the middle two columns to the GMC with $\langle n \rangle \sim 100\,cm^{-3}$, and the right two columns to the GMC with $\langle n \rangle \sim 200\,cm^{-3}$. In each pair of columns, the left one corresponds to solar metallicity ($Z = 1Z_\odot$) and the right one to sub-solar metallicity ($Z = 0.2Z_\odot$). In all cases, we consider a Galactic CR energy density ($\zeta' = 1$) and $G_\circ = 1$, normalized according to Draine (1978). It can be seen that $N(H_2)$ remains unchanged with decreasing Z and that $N(C\,I)$ and particularly $N(C\,II)$, do not decrease as dramatically as $N(CO)$ (note the scaling factors in the $0.2\,Z_\odot$ panels). As expected, the gas temperature slightly increases with decreasing Z, since the absence of metals reduces the overall cooling in the GMCs.

density in our computations). Atomic Carbon on the other hand remains abundant throughout the H_2-rich parts of the cloud, except for the low-metallicity gas where its abundance drops, but nevertheless remains generally higher than that of CO. The cloud mass fractions for which the [CO]/[H_2] abundance drops below 10^{-5} (i.e. 10 times below the average [CO]/[H_2] abundance in the Galaxy, making hard to use CO lines as H_2 gas mass tracers) are: 80 per cent, 55 per cent, and 30 per cent for $\langle n \rangle \sim 50$, 100, and $200\,cm^{-3}$, respectively, for

$Z = 1Z_\odot$, $K_{vir} = 1^2$, and $\zeta' = 1$. For the metal-poor case, the CO-poor cloud mass fraction becomes $\gtrsim 98$ per cent.

Nevertheless, unlike in our past higher density cloud models where most of $C\,II$ recombines into $C\,I$ (Bisbas et al. 2017), $C\,II$

---

[2]With $K_{vir} = (dV/dR)/(dV/dR)_{vir}$ a value of $K_{vir} = 1$ signifies self-gravitating clouds, see (Papadopoulos et al. 2014) for details.

now remains abundant for much of the mass of our low-density clouds (Fig. 1). Furthermore, classical photoelectric FUV heating, and the much lower average cooling of low-density gas ($\Lambda_{line} \propto n^2$), allows the gas to maintain higher temperatures $T_{kin} \sim (40 - 100)$ K for $\langle n \rangle \sim (50 - 100)\,cm^{-3}$, where the [C II] fine structure line is expected to be luminous.

Fig. 2 shows how the carbon cycle abundances change as a function of the total H column density for the four different ISM models. Here, we plot the average value of all three different clouds simultaneously. It can be seen that for the Galactic conditions (panel a), the molecular gas is CO-dominated for high column densities, as expected, while C remains abundant enough ([CI/CO] $\sim 0.1 - 0.3$) as to continue serving as a capable H_2 gas tracer along with CO (e.g. Papadopoulos et al. 2004). However, the molecular gas phase switches to a C I-dominated one in the lower metallicity case (panel b) and for $Z = 1 Z_{\odot}$ and $\zeta' = 30$ case (panel c). For even higher ζ', panel (d) shows a gas phase that becomes C II-dominated even at higher column densities (i.e. $\sim 6 \times 10^{21}\,cm^{-2}$) more typical for inner regions of molecular clouds.

Thus it may well be that, besides FUV photons, CRs also contribute in the making of (C II-line)-bright gas envelopes of (CO line)-invisible gas found around (CO line)-marked GMCs in the Galaxy (e.g. Pineda et al. 2013; Langer et al. 2014). Then these envelopes can be bright in both C II and C I lines, a possibility that should be investigated by sensitively imaging the latter in the C II-bright envelope regions of GMCs in the metal-rich inner parts of the Galaxy. The conditions for a widespread phase transition of H_2 gas from a CO-rich to a CO-poor/C I-rich phase can exist also for outer Galactic regions. Indeed as the star formation rate density becomes lower in the outer Galaxy, along with the intervening interstellar absorption they reduce the average FUV radiation field at large Galactocentric distances. CRs however can stream further out in the disc, and keep C I abundant in low-density molecular clouds.

There is already evidence for CO-poor gas in the Galaxy at large galactocentric radii from studies of otherwise CO-bright clouds selected in the Goddard–Columbia ^{12}CO survey. In these places an X_{CO} factor systematically larger by a factor of $\sim$2–3 with respect to its standard value at the inner Galaxy is found (Sodroski 1991). Other work using also CO-marked clouds finds that the diffuse H_2 clouds contain increasingly more H_2 mass at larger Galactocentric radii (Roman-Duval et al. 2016). These are the type of clouds that could contain a significant C I-rich/CO-poor phase according to our current study. Perhaps more significantly, the only search for the so-called CO-dark gas in our Galaxy, which is not using CO-selected H_2 clouds but dust extinction maps instead indicates that up to 55 per cent of the gas at large Galactocentric radii may be CO-dark (Chen et al. 2015). The same study finds that in certain regions the inferred CO-dark H_2 gas mass can reach up to four times the CO-luminous one.

We must note here that all our current arguments about CO-poor/C I-rich gas, as well as those that follow in the next sections, are phase-transition type of arguments. By this we mean that we are simply investigating the ISM conditions controlling the phase transition from a typically CO-rich to a CO-poor (and C I-rich) gas phase (with emphasis on the role of CRs, gas density, and metallicity), and the places where the conditions for such a phase transition can be fulfilled. In order to find how much H_2 mass is actually in such a gas phase, observations are indispensible. To this purpose we conclude this section by urging sensitive imaging of the two C I lines for the molecular gas in the Galaxy, and especially of its CO-poor yet C II-luminous phase.

2.1.1 The promise of ground-based high-frequency single dish telescope surveys

The *High Elevation Antarctic Terahertz Telescope* (HEAT), with a diameter of 60 cm, is a new high-frequency telescope now operating at Ridge A of the Antarctic plateau, with capabilities to observe both [C I] lines[3]. Its wide beam of $\sim$4.1$'$ at 492 GHz ([C I] 1–0) and 2.5$'$ at 809 GHz ([C I] 2–1) makes it appropriate for searching for low-brightness temperature (T_b) C I-rich molecular clouds in the Galaxy, where T_b([C I] 1–0)/T_b(CO 1–0) (hereafter T_b(C I)/T_b(CO)) drops to $\sim$0.15 in SF-quiescent regions (Papadopoulos et al. 2004, and references therein). An inventory of molecular gas in the Galaxy obtained using both [C I] lines and its comparison to the CO-rich and C II-rich gas can reveal whether a low-density C I-rich/CO-poor gas phase exists in the Milky Way, its spatial distribution, and temperature.

Other single dish submillimeter telescopes from excellent sites at the Atacama Plateau in North Chile (*APEX*, *NANTEN-2*, *and ASTE*) can be used to sensitively map C I (1–0) and/or (2–1) in a more targeted fashion for example along a continuous strip starting from the inner parts of a given Galactic molecular cloud and continuing well beyond its (CO/C I-line)-luminous regions, searching for C I-rich/CO-poor envelopes. The upcoming 5-m *Dome A Terahertz Explorer* (DATE5 Yang et al. 2013) in Dome-A of the Antarctic plateau will be able to perform a systematic survey across the Galactic plane with both good angular resolution and sensitivity, given its excellent condition for high-frequency observations (Shi et al. 2016). In Fig. 3, we show T_b(C I)/T_b(CO) ratio maps for our low-density ($\langle n \rangle \sim$50 cm^{-3}) inhomogeneous cloud model. These could be used to guide such an observational campaign in the Galaxy indicating the necessary C I/CO line relative brightness sensitivity levels.

2.2 Molecular gas outflows from galaxies

The discovery of strong H_2 outflows from galaxies, induced by AGN and/or starburst activity (Feruglio et al. 2010; Dasyra & Combes 2012; Cicone et al. 2012, 2014), shows that large amounts of molecular gas can be expelled from galaxies. It followed much earlier discoveries of huge cm-emitting synchrotron haloes around starburst galaxies (e.g. Seaquist & Odegard 1991; Colbert et al. 1996), indicating CRs outflows swept out from the star formation (SF) galaxy at bulk speeds $\gtrsim$1000 km s^{-1}. This could have significant effects since powerful molecular outflows are often discovered in those same starbursts where extended synchrotron haloes are found (e.g. Salak et al. 2013). Thus, the CO-destroying CRs could be swept along the molecular gas outflow itself. Moreover, by exerting large pressures on the molecular gas of starburst galaxies (even small gas ionization fractions can allow CR-gas coupling and momentum transfer from CRs to gas), CRs could even be driving these fast molecular outflows (Hanasz et al. 2013; Girichidis et al. 2016).

Low-density and gravitationally unbound molecular gas is to be expected in such galactic outflows, a result of Kelvin–Helmholtz instabilities and shear acting on the envelopes of denser clouds in the outflow. Such a gas phase could carry a significant mass fraction of the outflow, while remaining CO-invisible, because of large-scale CO destruction induced by the CRs carried within the same outflow. Large masses of low-density molecular gas could be present in galactic molecular gas outflows given the trend of progressively
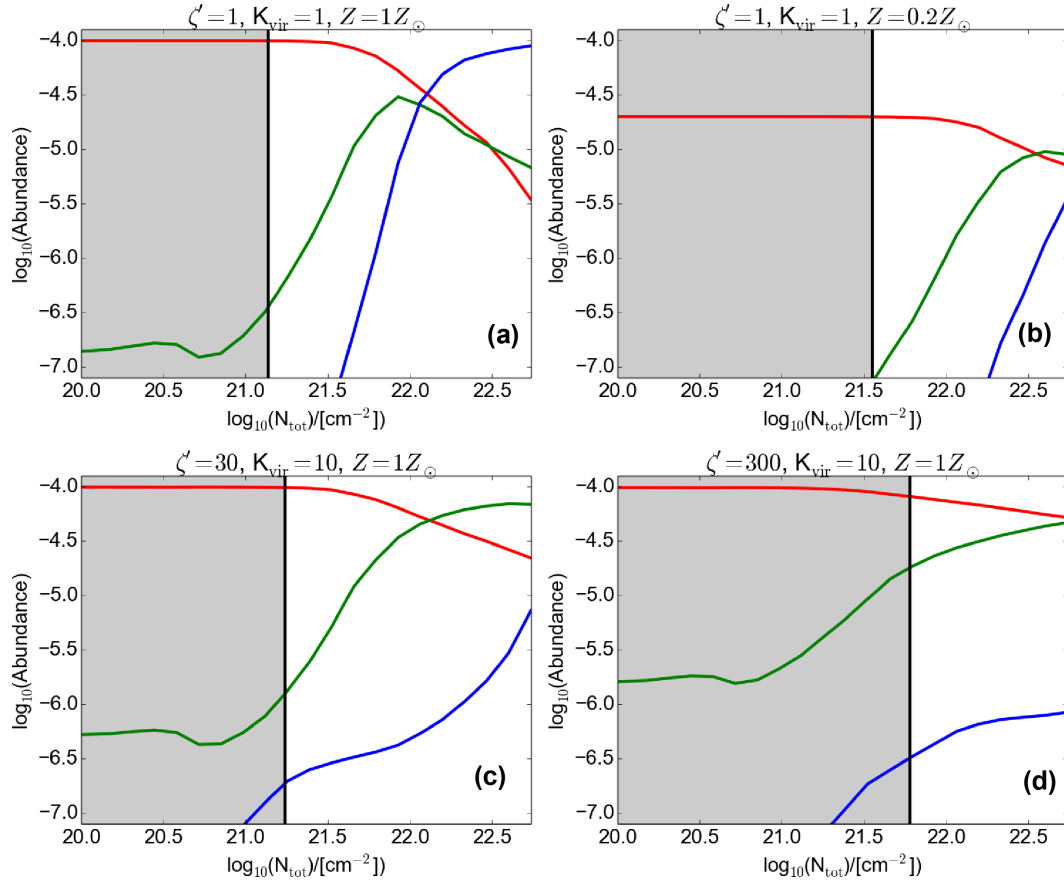
---

[3]http://soral.as.arizona.edu/HEAT/instrument/

Figure 2. The abundances of C II (red line), C I (green line), and CO (blue line) versus the total H-nucleus column density. Each line corresponds to the average value obtained from all three GMCs. Panels a and b correspond to the bound ($K_{vir} = 1$) GMC embedded in Galactic CR energy density ($\zeta' = 1$). We consider solar metallicity ($Z = 1Z_{\odot}$; panel a) and sub-solar metallicity ($Z = 0.2Z_{\odot}$; panel b). Panels c and d correspond to the unbound GMC ($K_{vir} = 10$) for solar metallicity. In panel c, the CR ionization rate is taken to be 30 times the Galactic ($\zeta' = 30$) and in panel d 300 times ($\zeta' = 300$). The vertical line shows the H I-to-H$_2$ transition (shaded area is atomic). We find that CO dominates as the main repository of carbon only for Galactic conditions (panel a) even as C remains abundant enough ([CI/CO] $\sim 0.1 - 0.5$ for the bulk of H$_2$ mass) as to remain a capable molecular gas mass tracer along with low-J CO lines.

larger amounts of molecular gas mass discovered in them, the lower the critical density of the line tracer used to reveal them is (Cicone et al. 2012). A CR-irradiation of the outflowing molecular gas by the relativistic plasma carried along with it thus points to the possibility of CO-poor/C I-rich molecular gas in powerful galactic outflows.

Using the magnetic field value found for the outflow in M 82 of $\langle B \rangle = 25\,\mu$G (Adebahr et al. 2013), and the equipartition assumption between magnetic field and CR energy densities, yields a CR energy density boost expected in such an outflow of $U_{CR} = (\langle B \rangle / \langle B_{Gal} \rangle)^2 \times U_{CR,\,Gal} \sim 17 \times U_{CR,\,Gal}$ (for $\langle B_{Gal} \rangle \sim 6\,\mu$G). Stronger magnetic fields of $\langle B \rangle \sim (35 - 40)\mu$G have been found in extended synchrotron haloes around galaxies (Laine & Beck 2008), corresponding to $U_{CR} \sim (34 - 44) \times U_{CR,\,Gal}$ for any concomitant H$_2$ gas phase outflowing along with the CRs. For our computations, we adopt $U_{CR} = 30 \times U_{CR,\,Gal}$ and $K_{vir} = 10$ corresponding to strongly unbound gas states expected in such galactic outflows.

Our results are shown in Fig. 4, from where it can be seen that CO is destroyed very effectively over the whole density range we consider in this work, while C I remains abundant. Thus sensitive C I 1–0, 2–1 imaging observations of galactic gas outflows could reveal significantly more H$_2$ gas mass than CO lines currently find. C II also remains abundant but starts strongly recombining to C I at the high-density end of $n \sim 200\,$cm^{-3}, as expected from our previous work (Bisbas et al. 2017).

In Fig. 5, we correlate the H$_2$ column density with the $T_b(C\,I)/T_b(CO)$ brightness ratio for the four different ISM environments we considered. As expected, high H$_2$ column densities (i.e. $N(H_2) \gtrsim 10^{22}\,$cm^{-2}) correspond to a small $T_b(C\,I)/T_b(CO)$ brightness ratio, implying that CO (1–0) is brighter than C I (1–0). From Figs 1 and 4, it can be seen that low $N(H_2)$ corresponds to gas temperatures that may exceed $\sim 50\,$K, particularly when the CR ionization rate is elevated (i.e. $\zeta' \gtrsim 30$). This may result in a local formation of CO via the OH channel (see Bisbas et al. 2017, for further details), which then increases $T_b(CO)$ and decreases $T_b(C\,I)$. This in turn, lowers their brightness ratio that we examine, resulting in a local minimum at $N(H_2) \sim 0.8 - 1 \times 10^{21}\,$cm^{-2} where FUV radiation is also important, as it can be seen from panels b and c of Fig. 5. For still higher CR energy densities (i.e. $\zeta' \sim 300$), all simulated GMCs become brighter in C I (1–0) than in CO (1–0).

3 RADIO GALAXIES: MOLECULAR GAS AND AGN-INJECTED COSMIC RAYS

The powerful jets of radio galaxies can carry CRs to great distances outside the galaxy where the radio-loud AGN resides, with the CRs also diffusing around the immediate confines of the jet to form magnetized bubbles (Guo & Mathews 2012). It is possible that such powerful jets can also entrain molecular gas from the ambient ISM
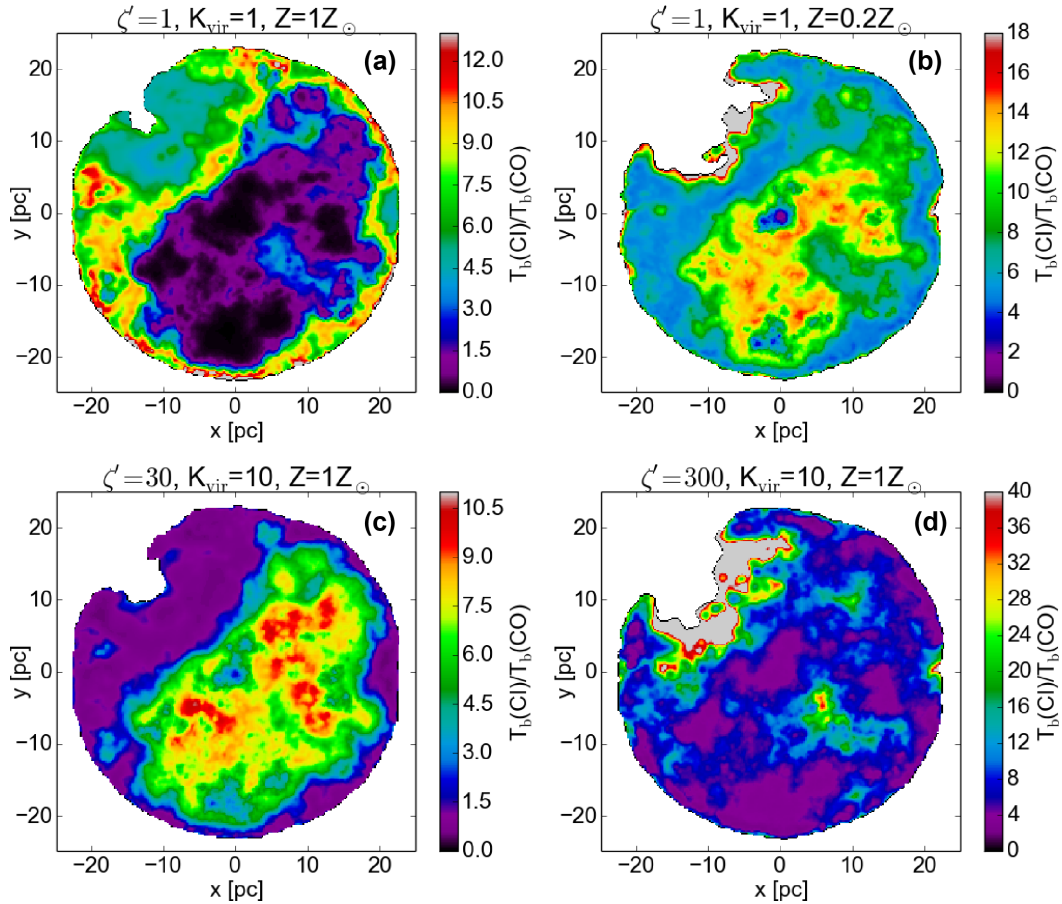
Figure 3. Maps of T$_b$(C I)/T$_b$(CO) (for the lowest 1−0 transition) brightness ratio of the GMC with $\langle n \rangle \sim 50$ cm^{-3} for different conditions. Panels a–d follow the ISM and GMC conditions described in Fig.2. In all cases we considered an isotropic interstellar radiation field with strength $G_\circ = 1$, normalized according to Draine (1978). The corresponding $N(H_2)$ distribution of panels a and b can be seen in the top row, left pair of columns of Fig. 1. The corresponding $N(H_2)$ distribution of panels c and d can be seen in the top row, left pair of columns of Fig. 4. We find that lower H$_2$ column densities [$N(H_2) \lesssim 10^{22}$ cm^{-2}, see Fig. 5] are in general brighter in CO in the Milky Way type of ISM conditions. In all other cases, we predict that these column densities will be brighter in [C I] (1–0) than in CO (1–0). Note also that in panels c and d, much lower column densities may become brighter in CO (1–0); this is because of the formation of CO via the OH channel as explained in detail in Bisbas et al. (2017), which locally increases the abundance of CO and hence its emission.

and drive molecular gas outflows, an effect already shown in the low-powered jets found in AGN-harbouring spirals like NGC 1068 (Lamastra et al. 2016), and NGC 4258 (Krause, Fendt & Neininger 2007). This is not so difficult to imagine, given that such jets are often launched from within gas-rich galaxies where the radio-loud AGN resides. Moreover, the heavily flared star-forming H$_2$ gas discs expected around AGN (Wada, Papadopoulos & Spaans 2009) can act as a constant source of molecular gas to be entrained by jets 'firing' from the AGN, given that the spins of disc and black hole rotation will not necessarily be aligned.

The interaction of cold gas with radio jets has already been studied theoretically and invoked to explain the H I outflows found in some powerful radio galaxies (Morganti, Tadhunter & Oosterloo 2005; Krause 2007), which have been since augmented by fast molecular gas outflows observed via the traditional method of CO lines (Morganti et al. 2015, 2016). Finally, significant amounts of molecular gas, the fuel of SF, driven out of radio-galaxies via jet-powered outflows provide a natural explanation for the so-called 'alignment effect' observed in many gas-rich high-redshift radio-galaxies (e.g. McCarthy et al. 1987; Pentericci et al. 2001).

Should molecular gas be 'caught' in a radio-jet driven outflow, it will be subjected to its withering CR-intense environ-

ment, which could quickly render it CO-poor/invisible. Moreover, a great deal of low-density gas (i.e. the phase where CR-induced and FUV induced CO destruction are most effective), is to be expected in such environments for the same reasons mentioned in Section 2.2 (to which perhaps MHD-driven shear should also be added).

Magnetic fields in radio-jets can be strong with $\langle B \rangle \sim (35 - 100)\mu G$ (Ostrowski 1998; Stawarz et al. 2005). Assuming equipartition between CR and magnetic field energy, yields CR energy densities within radio-jet environments of $U_{CR} \sim (35 - 280) \times \langle U_{CR,Gal} \rangle$. Thus, the CR energy density boost expected within jets and the areas near them approaches those expected in vigorous SF galaxies, even as the source of CRs is different. In Fig.4, we show images of the relative H I, H$_2$, CO, C I, and C II distributions for low-density clouds subjected to CR-irradiation environments of $U_{CR} = 300 \times \langle U_{CR,Gal} \rangle$, and in a strongly unbound state ($K_{vir} = 10$), that are plausible for gas found in radio-jets and radio-loud AGNs. CO is very effectively destroyed while both C I and C II remain abundant for such molecular gas (see Fig. 5d).

Nearby radio galaxies, such as Cen A and Minkowski's object, are excellent targets for detecting CO-poor/C I-rich molecular gas in jets and their vicinity. In Cen A, such gas may have already been
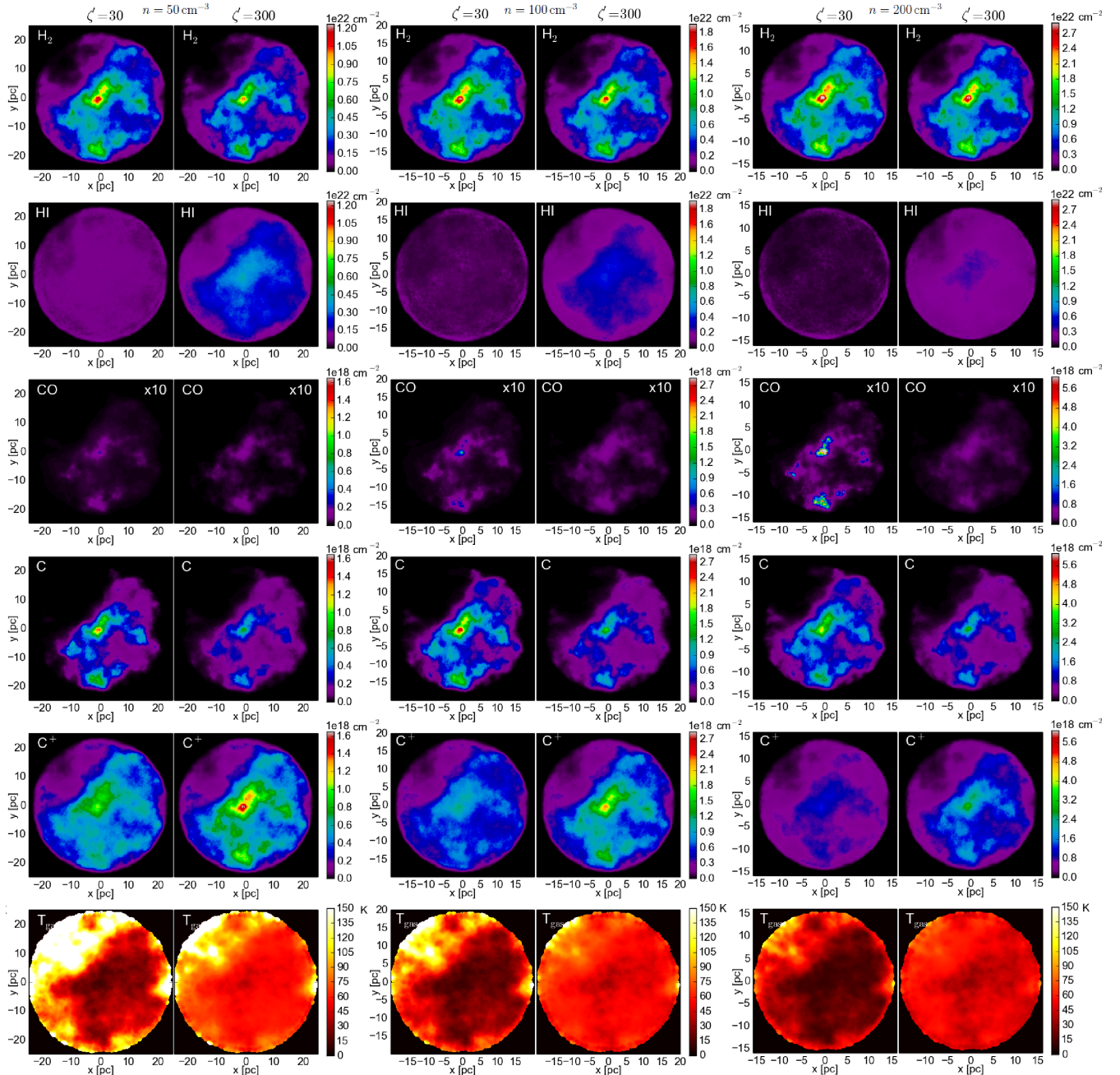
Figure 4. As in Fig. 1, but here the left column of each pair corresponds to an elevated CR energy density of $\zeta' = 30$ times the Galactic, and the right column to $\zeta' = 300$ times the Galactic. We consider $Z = 1Z_\odot$ and $G_\circ = 1$ everywhere. It can be seen that $N(H_2)$ remains remarkably unchanged at all times. $N(CO)$ is always smaller than $N(C\,\textsc{i})$ and $N(C\,\textsc{ii})$, which is in agreement with the findings of Bisbas et al. (2015, 2017). The gas temperature at the interior of the cloud increases with increasing ζ' and in the particular case of $\zeta' = 300$, it is approximately uniform ($T_{gas} \sim 50 - 70\,K$) regardless of the local density, n. The conditions presented here are expected to be found in radio-galaxies.

detected, even if its bright C I emission has been attributed to PDRs rather than CRDRs (Israel et al. 2017).[4]

---

[4]*Relative* molecular line ratios can always be fitted with PDRs (e.g. van der Werf et al. 2010), yet the decisive test whether PDRs or CRDRs/XDRs are responsible for any observed extragalactic lines must use the relative gas mass fractions of warm/dense gas and warm dust (see Bradford et al. 2003; ; van der Werf et al. 2010; Papadopoulos et al. 2014). No such tests have been done for the C I-bright molecular gas in Cen A.

In the case of Minkowski's object, sensitive CO observations detected only a small CO-marked H_2 gas reservoir fueling the star formation observed along its jet, making this object an outlier of the Schmidt-Kennicutt (S-K) relation (SalomSalomé, Salomé & Combesé et al. 2015; Lacy et al. 2017). Sensitive [C I] (1–0) imaging of this galaxy is particularly promising for detecting molecular gas that may have been rendered CO-invisible by the high U_{CR} expected in its radio jet. Similar observations of radio galaxies at high redshifts are even more promising, because in the early Universe these galaxies reside in very H_2-rich hosts with
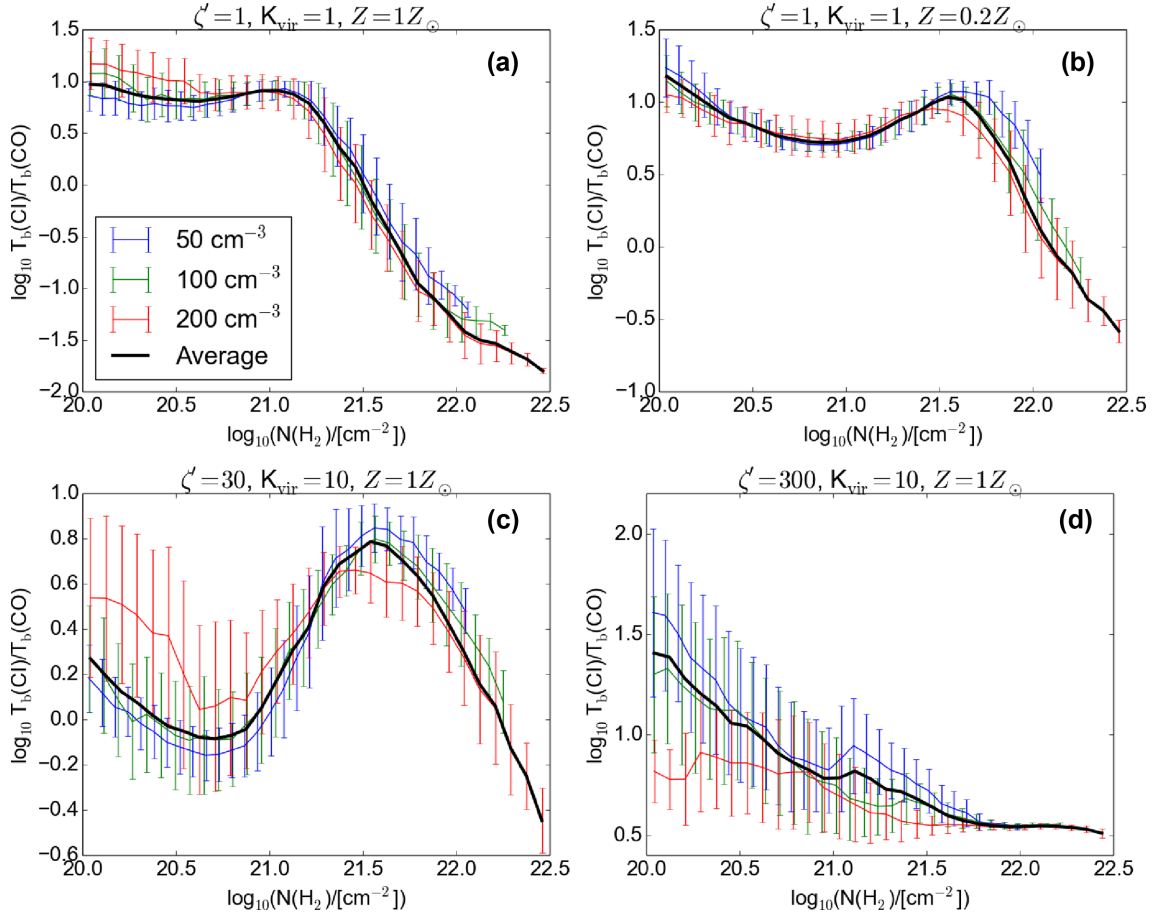
Figure 5. Correlation of $N(H_2)$ with $T_b(C\,I)/T_b(CO)$ (for the lowest 1–0 transition) for all different ISM environments we explore. The error-bar corresponds to 1σ standard deviation. Lines in blue colour corresponds to the GMC with $\langle n \rangle \sim 50\,\mathrm{cm}^{-3}$, green with $\sim 100\,\mathrm{cm}^{-3}$, and red with $\sim 200\,\mathrm{cm}^{-3}$. The black solid line shows the average value of the $T_b(C\,I)/T_b(CO)$ ratio from all three different GMCs in each case. The local minimum in panels b and c are due to the formation of CO via the OH channel (Bisbas et al. 2017), since in this regime the gas temperature is $T_{gas} \gtrsim 50\,\mathrm{K}$ (see Fig. 4). Note that for panels b, c, and d, we always obtain $T_b(C\,I)/T_b(CO) \gtrsim 0.1$.

plenty of gas to be entrained/impacted by their powerful jets. Finally, [C I] (1–0) and even (2–1) line imaging observations can be conducted in the distant Universe with modest T_{sys} since their frequencies will be redshifted to more transparent parts of the Earth's atmosphere.

4 MS GALAXIES: CRS AND LOW-METALLICITY GAS

A mostly CR-regulated average [CO]/[H₂] abundance in the ISM of MS galaxies and the possibility of large fractions of their molecular gas mass having their CO destroyed (with adverse effects on the calibration attempts of their X_{CO}-factor (e.g. Genzel et al. 2012; Carleton et al. 2017)) have been described by Bisbas et al. (2015, 2017). Our current models of lower density gas clouds, reinforce this view by demonstrating that the conditions for a phase transition towards very CO-poor gas remain favorable for low densities even for Galactic or only modestly elevated levels of CR energy densities. For low-metallicity gas, the effects of CO destruction are dramatic (Fig. 1), and could explain the lack of total CO emission seen in some metal-poor MS galaxies (Genzel et al. 2012). Such CO-dark molecular gas may also exist in the outer regions of MS galaxies, which otherwise show CO-bright and metal-rich molecular gas in their inner SF regions.

One may ask whether significant amounts of lower density molecular gas can indeed exist in such vigorous SF discs. Given that star formation is a low-efficiency process, both on the mass scale of individual molecular clouds and that of galaxy-sized reservoirs, we can expect that large amounts of non-SF molecular gas will always be present in SF galaxies, either in their disc, or expelled out by SF feedback (e.g. the massive non-SF H₂ gas reservoir in the outer regions of M 82). With CRs able to 'leak' out of the SF areas along molecular gas outflows and beyond the SF disc, they can subject non-SF low-density gas to significant levels of CR irradiation, destroying its CO and replacing with C I and C II. Sensitive C I line imaging of such systems can show whether this is so. Nevertheless at redshifts of $z \gtrsim 4$, C II line imaging will be the most effective in revealing such gas.

4.1 C I line imaging and a critical brightness limit

There are now several *PdBI* and *ALMA* C I (1–0), (2–1) line observations of galaxies in the distant Universe (Walter et al. 2011; Zhang et al. 2014; Gullberg et al. 2016; Popping et al. 2017; Bothwell et al. 2017; Emonts 2017) as well as local ones using *Herschel* (Jiao et al. 2017). In all cases, the galaxies are either unresolved or only marginally resolved in [C I] line emission. Such observations do not yet allow a detailed study of relative distributions of C I versus CO

1–0 emission in galaxies, since unresolved or marginally resolved emission will always be dominated by the warm and dense star-forming H_2 gas (where both CO and C I are abundant). However, Krips et al. (2016) recently provided a $3''$ resolution of CO(1–0) and [C I] (1–0) for the SF galaxy NGC 253. Intriguingly, recent high-resolution ALMA imaging of [C I] (1–0) lines in a local Luminous Infrared Galaxy (LIRG) shows significant differences between the CO and C I-bright H_2 gas distribution (Zhang et al. *in prep.*).

High-resolution imaging of CO and [C I] (1–0), (2–1) lines of local LIRGs is necessary to compare their emission distribution in detail and deduce the corresponding H_2 mass distributions. The resolution however must be high enough to separate the more compact SF molecular gas distributions from the more extended SF-quiescent, and perhaps lower density gas reservoirs. The strongest requirement for such imaging is then placed by the conditions in latter where observations yield brightness temperature ratios $T_b(C\,I)/T_b(CO) \sim 0.15$ (Papadopoulos et al. 2004, and references therein). From Fig. 5 we can see that a C I/CO $(J = 1 - 0)$ relative brightness cutoff of $T_b(C\,I)/T_b(CO) \sim 0.10$ is adequate to encompass all the H_2 gas in the clouds, irrespective of its thermal/chemical state and their intrinsic average [CO]/[C I] ratio. Predictably, it is the denser/colder inner regions of our low-density cloud models (and where the average $N(H_2)$ is the highest), where this ratio drops to its lowest values, as is indeed found by simulations and observations of cold/low-density non-SF molecular cloud regions in the Galaxy (Papadopoulos et al. 2004; Offner et al. 2014; Lo et al. 2014; Glover & Clark 2016).

It is perhaps more beneficial to conduct such high brightness sensitivity C I (and CO) line imaging for SF discs in the more distant Universe (e.g in the discs of MS and submillimeter galaxies, radio galaxy environments) as to take advantage of the lower T_{sys} *ALMA* values for the C I redshifted frequencies. Even at $z \gtrsim 0.4$, the C I (1–0) frequency already shifts to $\lesssim 350$ GHz, where the atmosphere becomes much more transparent and detectors less noisy. Furthermore, it is during earlier cosmic epochs (and thus distances) when galaxies become more H_2-rich, while the CRs generated by their elevated Star Formation Rates (SFRs) can induce large-scale CO destruction leaving behind C I-rich gas.

5 CONCLUSIONS

The astrochemistry that demonstrated the critical role of CRs in regulating the average [CO]/[H_2] abundance for the bulk of the molecular gas in SF galaxies (except in localised surface PDRs near O,B stars) indicates that CO-poor/C I-rich can exist not only in the highly CR-irradiated ISM environments of starbursts but also in environments with much lower levels of CR-irradiation, if the average molecular gas density is low. A low-density molecular gas phase with CR irradiation levels high enough to render it very CO-poor and C I/C II-rich can be found in a number of places in the Universe, namely:

(i) Low-density envelopes around the CO-rich parts of ordinary molecular clouds in the Milky Way,

(ii) Molecular gas outflows from galaxies, induced by starburst and/or AGNs,

(iii) In MS galaxies both in their metal-rich and metal-poor regions (in the latter ones CR and FUV irradiation penetrate deep in H_2 destroying the CO tracer molecule).

(iv) In regions inside and around radio-jets and perhaps even near the cores of powerful radio galaxies.

Sensitive C I line observations of such environments can perhaps find more molecular gas mass than the standard low-J CO line

observations, provided a relative brightness temperature ratio of $T_b(C\,I)/T_b(CO) \sim 0.10$ (for $J = 1 - 0$) is reached in well-resolved images. GMCs in the Galaxy, distant MS, and submillimeter galaxies, as well as areas around radio galaxies and their jets are all excellent targets for this kind of imaging. In the later case, Minkowski's object as well as Cygnus A are some of the most prominent radio-loud objects for such observations in the local Universe.

REFERENCES

Adebahr B., Krause M., Klein U., Weżgowiec M., Bomans D.J., Dettmar R.-J., 2013, A&A, 555, A23
Andersson B.-G., Wannier P. G., 1993, ApJ, 402, 585
Bialy S., Sternberg A., 2015, MNRAS, 450, 4424
Bialy S., Sternberg A., 2016, ApJ, 822, 83
Bialy S., Burkhart B., Sternberg A., 2017, ApJ, 843, 92
Bisbas T. G., Bell T. A., Viti S., Yates J., Barlow M. J., 2012, MNRAS, 427, 2100
Bisbas T. G., Papadopoulos P. P., Viti S., 2015, ApJ, 803, 37
Bisbas T. G., van Dishoeck E. F., Papadopoulos P. P., Szűcs L., Bialy S., Zhang Z., 2017, ApJ, 839, 90
Bolatto A. D., Jackson J. M., Ingalls J. G., 1999, ApJ, 513, 275
Bothwell M. S. e et al., 2017, MNRAS, 466, 2825
Bradford C. M., Nikola T., Stacey G. J., Bolatto A.D., Jackson J.M., Savage M.L., Davidson J.A., Higdon S.J., 2003, ApJ, 586, 891
Bryant P. M., Scoville N. Z., 1996, ApJ, 457, 678
Carleton T. et al., 2017, MNRAS, 467, 4886
Chen B.-Q., Liu X.-W., Yuan H.-B., Huang Y., Xiang M.-S., 2015, MNRAS, 448, 2187
Cicone C., Feruglio C., Maiolino R., Fiore F., Piconcelli E., M enci N., Aussel H., Sturm E., 2012, A&A, 543, A99
Cicone C. et al., 2014, A&A, 562, A21
Colbert E. J. M., Baum S. A., Gallimore J. F., O'Dea C.P., Lehnert M.D., T svetanov J.I., Mulchaey J.S., Caganoff S., 1996, ApJS, 105, 75
Dasyra K. M., Combes F., 2012, A&A, 541, L7
Dickman R. L., Snell R. L., Schloerb F. P., 1986, ApJ, 309, 326
Draine B. T., 1978, ApJS, 36, 595
Emonts B., 2017, Formation and Evolution of Galaxy Outskirts, 321, 348
Feruglio C., Maiolino R., Piconcelli E., M enci M., Aussel H., L amastra A., F iore F., 2010, A&A, 518, L155
Genzel R. et al., 2012, ApJ, 746, 69
Girichidis P. et al., 2016, ApJ, 816, L19
Glover S. C. O., Clark P. C., 2016, MNRAS, 456, 3596
Gullberg B. et al., 2016, A&A, 591, A73
Guo F., Mathews W. G., 2012, ApJ, 756, 181
Hanasz M., Lesch H., Naab T., Gawryszczak A., K owalik K., Wóltański D., 2013, ApJ, 777, L38
Heyer M., Dame T. M., 2015, ARA&A, 53, 583
Hollenbach D. J., Tielens A. G. G. M., 1999, Rev. Mod. Phys., 71, 173
Israel F. P., Güsten R., Meijerink R., Requena-Torres M. A., Stutzki J., 2017, A&A, 599, A53
Jiao Q., Zhao Y., Zhu M., Lu N., Gao Y., Z hang Z.-Y., 2017, ApJ, 840, L18
Jura M., 1975a, ApJ, 197, 575
Jura M., 1975b, ApJ, 197, 581
Krause M., 2007, New Astron. Rev., 51, 174
Krause M., Fendt C., Neininger N., 2007, A&A, 467, 1037

Krips M. et al., 2016, A&A, 592, L3

Lacy M, Croft S., Fragile C., Wood S., Nyland K., 2017, ApJ, 838, 146

Laine S., Beck R., 2008, ApJ, 673, 128

Lamastra A. et al., 2016, A&A, 596, A68

Langer W. D., Velusamy T., Pineda J. L., Willacy K., Goldsmith P. F., 2014, A&A, 561, A122

Lo N. et al., 2014, ApJ, 797, L17

Madden S. C., Poglitsch A., Geis N., Stacey G. J., Townes C. H., 1997, ApJ, 483, 200

Maloney P., Black J. H., 1988, ApJ, 325, 389

McCarthy P. J., van Breugel W., Spinrad H., Djorgovski S., 1987, ApJ, 321, L29

Meijerink R., Spaans M., Loenen A. F., van der Werf P. P., 2011, A&A, 525, A119

Meixner M., Tielens A. G. G. M., 1993, ApJ, 405, 216

Morganti R., Tadhunter C. N., Oosterloo T. A., 2005, A&A, 444, L9

Morganti R., Oosterloo T., Oonk J. B. R., Frieswijk W., Tadhunter C., 2015, A&A, 580, A1

Morganti R., Oosterloo T., Oonk J. B. R., Santoro F., Tadhunter C., 2016, A&A, 592, L9

Offner S. S. R., Bisbas T. G., Viti S., Bell T. A., 2013, ApJ, 770, 49

Offner S. S. R., Bisbas T. G., Bell T. A., Viti S., 2014, MNRAS, 440, L81

Ostrowski M., 1998, A&A, 335, 134

Padoan P., Nordlund, Å., 2002, ApJ, 576, 870

Pak S., Jaffe D. T., van Dishoeck E. F., Johansson L. E. B., Booth R. S., 1998, ApJ, 498, 735

Papadopoulos P. P., 2010, ApJ, 720, 226

Papadopoulos P. P., Thi W.-F., Viti S., 2002, ApJ, 579, 270

Papadopoulos P. P., Thi W.-F., Viti S., 2004, MNRAS, 351, 147

Papadopoulos P. P. et al., 2014, ApJ, 788, 153

Pentericci L., McCarthy P. J., Röttgering H. J. A., M iley G.K., van Breugel W.J.M., Fosbury R. et al., 2001, ApJS, 135, 63

Pineda J. L., Langer W. D., Velusamy T., Goldsmith P. F., 2013, A&A, 554, A103

Popping G. et al., 2017, A&A, 602, A11

Roman-Duval J., Heyer M., Brunt C. M., Clark P., K lessen R., Shetty R., 2016, ApJ, 818, 144

Sakamoto S., Hasegawa T., Handa T., Hayashi M., Oka T., 1997, ApJ, 486, 276

Salak D., Nakai N., Miyamoto Y., Yamauchi A., Tsuru T. G., 2013, PASJ, 65, 66

Salomé Q., Salomé P., Combes F., 2015, A&A, 574, A34

Seaquist E. R., Odegard N., 1991, ApJ, 369, 320

Shaya E. J., Federman S. R., 1987, ApJ, 319, 76

Shi S.-C. et al., 2016, NatAs, 1, 1

Shull J. M. et al., 2000, ApJ, 538, L73

Sodroski T. J., 1991, ApJ, 366, 95

Solomon P. M., Downes D., Radford S. J. E., 1992, ApJ, 387, L55

Solomon P. M., Downes D., Radford S. J. E., Barrett J. W., 1997, ApJ, 478, 144

Spaans M., van Dishoeck E. F., 1997, A&A, 323, 953

Stawarz, Ł., Siemiginowska A., Ostrowski M., Sikora M., 2005, ApJ, 626, 120

van der Werf P. P. et al., 2010, A&A, 518, L42

van Dishoeck E. F., Black J. H., 1986, ApJS, 62, 109

Wada K., Papadopoulos P. P., Spaans M., 2009, ApJ, 702, 63

Walch S., Whitworth A. P., Bisbas T. G., Hubber D. A., Wünsch R., 2015, MNRAS, 452, 2794

Walter F., Weiß A., Downes D., Decarli R., Henkel C., 2011, ApJ, 730, 18

Wolfire M. G., Hollenbach D., McKee C. F., 2010, ApJ, 716, 1191

Yang J., Zuo Y.-X., Lou Z., Cheng J.-Q., Zhang Q.-Z., Shi S.-C., Huang J.-S., Yao Q., Wang Z., 2013, RAA, 13, 1493

Young J. S., Scoville N. Z., 1991, ARA&A, 29, 581

Zhang Z.-Y. et al., 2014, A&A, 568, A122

This paper has been typeset from a TEX/LATEX file prepared by the author.